Nexus between Quantum Criticality and Phase Formation in $U(Ru_{1-x}Rh_x)_2Si_2$

K. H. Kim,[1,*] N. Harrison,[1] H. Amitsuka,[2] G. A. Jorge,[1] M. Jaime,[1] and J. A. Mydosh[3,4]

[1]*National High Magnetic Field Laboratory, Los Alamos National Laboratory, MS E536, Los Alamos, New Mexico 87545, USA*

[2]*Graduate School of Science, Hokkaido University, N10W8 Sapporo 060-0810, Japan*

[3]*Kamerlingh Onnes Laboratory, Leiden University, 2300RA Leiden, The Netherlands*

[4]*Max-Planck-Institut für Chemische Physik fester Stoffe, 01187 Dresden, Germany*

(Received 13 February 2004; published 10 November 2004)

Simplification of the magnetic field-versus-temperature phase diagram and quantum criticality in URu_2Si_2 dilutely doped with Rh are studied by measuring the magnetization and resistivity in magnetic fields of up to 45 T. For $x = 4\%$, the hidden order is completely destroyed, leaving a single field-induced phase II. A correlation between the field dependence of this phase and that of the quantum critical point, combined with the suppression of the T^2 coefficient of the resistivity within it, implicates field-tuned quantum criticality as an important factor in phase formation.

DOI: 10.1103/PhysRevLett.93.206402 PACS numbers: 71.45.Lr, 71.18.+y, 71.20.Ps

Quantum criticality is becoming increasingly recognized as a controlling factor in the creation of novel phases [1–4]. In addition to quantum fluctuations providing opportunities for quasiparticle pairing, quasiparticle divergences associated with quantum criticality itself can potentially cause the metallic phase to become unstable [3–6]. There exist several examples where novel (mostly superconducting) phases appear within close proximity of a critical pressure (or dopant concentration) p at which a quantum critical point (QCP) is realized [7–9]. However, proof of a causality link between quantum criticality and phase formation remains a formidable experimental challenge. Even its microscopic origin remains subject to theoretical debate [1]. This is equally true for antiferromagnetic QCPs [10], metamagnetic transitions [11], and proposed QCPs concealed beneath the superconducting phase of the cuprates [12].

URu_2Si_2 is an example of a system where signatures of quantum criticality appear at very strong magnetic fields $B \sim 40$ T [13,14], suggestive of a QCP concealed beneath a complex region of interconnecting phases [13,15]. Because of the possible involvement of magnetic field-induced quantum criticality in the creation of some (or all) of the phases, this system could constitute an important paradigm for future models. The order parameters involved nevertheless remain unidentified [13,15], and attempts to understand the phase diagram under a magnetic field are compounded by a "hidden order" (HO) parameter [16], which terminates in the same region of the phase diagram where quantum criticality occurs [17,18].

In this Letter, we show that the dilute substitution of Rh in place of Ru, so as to yield $U(Ru_{1-x}Rh_x)_2Si_2$, provides an opportunity to study quantum criticality in the absence of HO [19,20]. When $x = 4\%$, the HO parameter no longer exists [19,20], giving way to a heavy-Fermi liquid at low magnetic fields. The central message of this Letter is that Rh doping yields a single field-induced phase, previously referred to as "phase II" [13], with a clear nexus between phase II and the QCP. The field at which the highest critical temperature is observed, B_{II}, and the field at which the QCP occurs, B_{QCP}, move together with x. Evidence for quantum criticality is observed outside the ordered phase, being consistent with a single point (hidden beneath phase II) at which the effective Fermi energy of the quasiparticles $\varepsilon_F = \hbar^2 k_F^2/2m^*$ extrapolates to zero from both the high and low magnetic field limits.

The present study is performed on single crystals of $U(Ru_{1-x}Rh_x)_2Si_2$ of composition $x = 2\%$, 2.5%, 3%, and 4%, with limited supplementary measurements performed on the $x = 0$ and $x = 1\%$ systems to verify continuity with x and consistency with previous measurements [13,14,19]. Single crystals are grown using the same Czochralski method as used by Yokoyama *et al.* [20]. Measurements of the magnetization M are performed using a long-pulse magnet [14], while measurements of the resistivity ρ are performed in the 45 T hybrid magnet in Tallahassee [13]. Supplementary measurements of ρ, made using the pulse magnet, provide a reliable means for verifying that isothermal conditions are achieved throughout [17]. Temperatures T down to 400 mK are achieved using a plastic ^{3}He refrigerator. Identical methods to those used in the case of pure URu_2Si_2 for extracting phase boundaries, the Fermi crossover temperature T^*, locus $[T_{\rho\,\max}, B]$ of the magnetoresistivity maximum $\rho_{\max}$, and the low temperature T^2 coefficient A of ρ [13,14] are repeated here for each x.

Figure 1 shows the evolution of the phase diagram and quantum criticality in $U(Ru_{1-x}Rh_x)_2Si_2$ with x, where different ordered phases are shaded for clarity. For $x = 2\%$, the phase diagram is similar to that obtained for pure URu_2Si_2, but with "phase V" absent. In URu_2Si_2, the HO phase dominates the low temperature thermodynamics over a wide interval in field, while phase III was considered as a possible reentrant HO phase [14]. Phase II is a much weaker feature that nevertheless appears in trans-

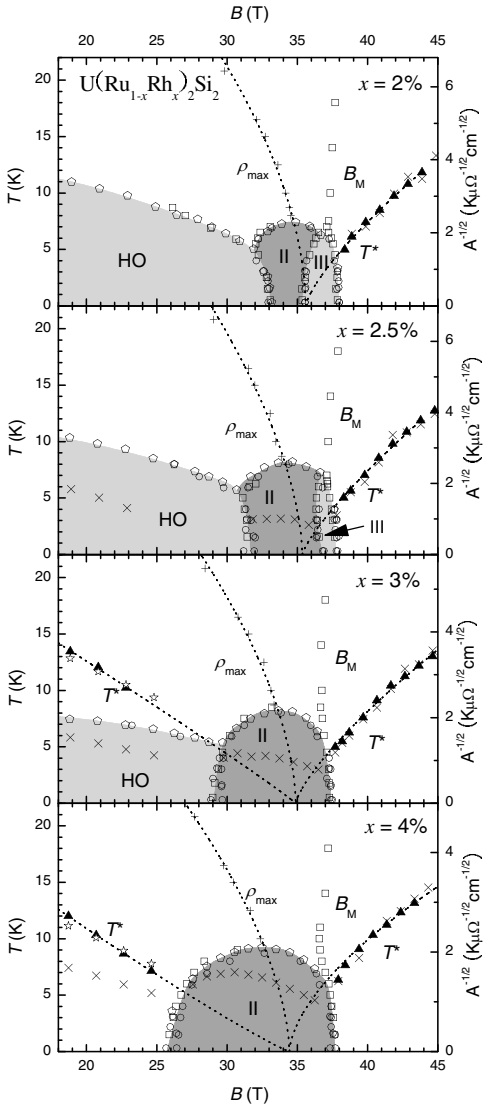

FIG. 1. High magnetic field region of the phase diagram of $U(Ru_{1-x}Ru_x)_2Si_2$ for compositions $x = 2\%$, 2.5%, 3%, and 4%, in which the ordered phases are shaded for clarity. Open squares correspond to maxima in χ, open circles (pentagons) correspond to sharp extremities in $\partial\rho/\partial B$ ($\partial\rho/\partial T$). "+" symbols delineate the T and B coordinates of the maxima $\rho_{\max}$ in the magnetoresistivity, while up-triangles delineate the crossover T^* from low temperature T^2 resistivity behavior to high temperature sublinear behavior. Dotted lines correspond to fits to the function $T(B) \propto |B - B_{\rm QCP}|^{\alpha}$, as described in the text. "×" symbols represent $A^{-1/2}$ plotted using the right-hand axes, while "★" symbols represent the same data rescaled for $B < B_{\rm QCP}$ as described in the text.

port [13], ultrasound velocity [15], and specific heat [17,18] measurements. Open symbols delineate what we propose to be direct evidence for phase transitions as found in URu_2Si_2 [13,14]. Squares represent maxima in the differential susceptibility $\chi = \mu_0 \partial M/\partial B$ that usually occur at first order phase transitions [21] or crossovers, while circles and pentagons represent sharp extremities in the derivatives $\partial\rho/\partial B$ and $\partial\rho/\partial T$, respectively.

The phase diagram already starts to change profoundly upon making an incremental change in x from 2% to 2.5%. Most notably, the region occupied by phase II expands with its corresponding phase transition features in $\partial\rho/\partial T$, $\partial\rho/\partial B$, and χ becoming stronger. By contrast, the HO phase is suppressed, especially at low magnetic fields [19], while phase III becomes very narrow, developing a "rabbit ear" shape. At $x = 3\%$, phase III has abruptly disappeared, while phase II encroaches deeper into the region previously occupied by the HO phase, whose transition has become considerably weakened. Once $x = 4\%$, the data are consistent with the vanishing of the HO phase reported by Yokoyama *et al.* [20], leaving phase II as a single field-induced phase.

Phase III (the "reentrant hidden order" phase) was proposed to be the product of quantum criticality in previous magnetization studies [14]. The present study indicates that this appears also to be true for phase II. The QCP, which corresponds to the convergence of dotted lines obtained upon fitting and extrapolating physical parameters T^*, A, and $T_{\rho\,\max}$, is concealed beneath phase III in pure URu_2Si_2 but is now submerged beneath phase II for $x \gtrsim 2\%$ in Fig. 1. Evidence for quantum criticality is obtained from the temperature dependence of the resistivity. A first, though indirect, indication of field-induced quantum criticality is the emergence of a broad maximum $\rho_{\max}$ in the magnetoresistivity at $[T_{\rho\,\max}, B]$ [13,22], delineated by + symbols in Fig. 1, which systematically narrows and shifts to higher magnetic fields on decreasing T. This is also true for pure URu_2Si_2 [13], for which $[T_{\rho\,\max}, B]$ can be fitted to a generic function of the form $T_{\rho\,\max} \propto |B - B_{\rm QCP}|^{\alpha}$, in accordance with the scaling theory of quantum phase transitions [23]. Fits of this function (dotted line) in the case of the Rh-doped samples in Fig. 1 yield $\alpha \approx 0.60 \pm 0.05$ and the values for $B_{\rm QCP}$ shown in Fig. 2(a).

The collapse of $\varepsilon_{\rm F}$ on approaching $B_{\rm QCP}$ provides more direct evidence for quantum criticality, which can be inferred from both the exponent n and the prefactor A of ρ on fitting its T dependence to $\rho(T) = \rho_0 + AT^n$ for $0.6 \lesssim T \lesssim 3$ K. In the regions outside the ordered phases, as in the case of pure URu_2Si_2, n crosses over from a value of $n \approx 2$ to $n \leq 1$ at T^*. This is seen directly as a broad maximum in the derivative $\partial\rho/\partial T$, represented by filled

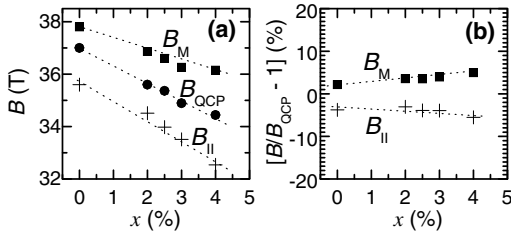

FIG. 2. (a) Comparison of the trends in $B_{\rm II}$, $B_{\rm QCP}$, and $B_{\rm M}$ as x is varied. (b) Percentage differences between $B_{\rm II}$ and $B_{\rm QCP}$ and $B_{\rm M}$ and $B_{\rm QCP}$.

triangle symbols in Fig. 1. This crossover is observed at fields both above and below B_{QCP} for $x \geq 3\%$ owing to the suppression of the HO. Fits of the function $T^* \propto |B - B_{QCP}|^{\alpha}$ to the T^* data yield $\alpha \approx 0.70 \pm 0.05$ for $B > B_{QCP}$ and $\alpha \approx 1.0 \pm 0.1$ for $B < B_{QCP}$. Since Fermi liquid behavior with $n = 2$ is conditional upon $k_B T < \varepsilon_F$, T^* could correspond to the situation in which the width of the derivative of the Fermi-Dirac distribution function $\sim k_B T$ approximately matches ε_F. Combining the Sommerfeld expression of the electronic specific heat with the Kadowaki-Woods [24] ratio $R_{KW} = A/\gamma^2$ yields $\varepsilon_F \approx \pi^2 k_B^2 \aleph N_A \sqrt{R_{KW}/A}$, where $\aleph \approx 0.016$ [25] is the volume of the Fermi surface divided by that of the Brillouin zone. On inserting $A^{-1/2} \sim 3\ \mathrm{K}\,\mu\Omega^{-1/2}\,\mathrm{cm}^{-1/2}$ for $x = 4\%$ at 18 and 45 T in Fig. 1 ($\times$ symbols) into this expression, we obtain $\varepsilon_F/k_B \approx 12$ K, in fair agreement with the observed values of T^* (triangles) at 18 and 45 T in Fig. 1. In fact, a general scaling proportionality $T^* \propto A^{-1/2} \propto \varepsilon_F$ can be seen to apply for all B in Fig. 1, although rescaling of $A^{-1/2}$ by 2.2 and 1.5 is required at fields $B < B_{QCP}$ for $x = 3\%$ and 4%, respectively ($\bigstar$ symbols in Fig. 1). Since A depends on the number of particles as well as their effective masses, this rescaling between $B < B_{QCP}$ and $B > B_{QCP}$ is suggestive of a change in Fermi surface topology at B_{QCP} [25].

The ease by which simple power laws proportional to $|B - B_{QCP}|^{\alpha}$ are able to fit the field dependence of $T_{\rho\,\max}$, T^*, and $A^{-1/2}$ (scaled) in Fig. 1, with different exponents α but a common value of B_{QCP}, is strongly suggestive of a single QCP hidden beneath phases II and/or III at all concentrations $0 \leq x \leq 4\%$. A probable causality link between this QCP and phase II becomes apparent in Fig. 2(a) on comparing B_{QCP} with B_{II}, the field at which the transition temperature into phase II is highest. Both move together as x is varied, with a difference in field of a few percent between them being approximately independent of x in Fig. 2(b). The same is true for the metamagnetic crossover field B_M, which we estimate here by extrapolating the high temperature maximum in χ to the $T = 0$ intercept. While there is a clear correlation among B_{QCP}, B_{II}, and B_M, the existence of an approximate 2%–3% discrepancy in field between B_{QCP} and B_M is surprising. These two quantities are considered to be the same in the quantum critical end point model [11,13,14,22].

The quantum critical end point scenario was proposed to address the apparent absence of symmetry breaking at the $T = 0$ metamagnetic transition and its transformation into a mere crossover at finite temperatures [11,22]. Models that consider the magnetization as the order parameter provide a good description of the behavior seen in $Sr_3Ru_2O_7$ [11,22] but have yet to account for large discontinuous changes in Fermi surface topology (by as much as one electron per Ce or U atom) that occur in itinerant f-electron metamagnets such as $CeRu_2Si_2$ [26] (as might also occur at B_M in URu_2Si_2 [14]). This aspect of the physics might instead be captured by models that propose quantum criticality to be driven by changes in "topological order" between two different Fermi liquid states with different Fermi surface topologies and different quasiparticles [27]. In such a model, localization of the f electrons within one of the Fermi liquid states then becomes a precondition for magnetic order (whether this involves their antiferromagnetic or ferromagnetic alignment), with other factors ultimately determining the point at which ordering takes place, thereby relaxing the requirement that $B_{QCP} \equiv B_M$.

While the microscopic origin of quantum criticality in heavy fermion metamagnets remains subject to debate, Figs. 1 and 2 do nevertheless provide evidence for phase II forming as a means of avoiding the QCP at B_{QCP}. In addition to the common trend among B_{QCP}, B_M, and B_{II} in Fig. 2, the formation of phase II appears to quench the divergence in A in Fig. 3 that would otherwise occur in its absence. The dotted line fits imply that we would expect $A^{-1/2}$ and T^* to collapse to zero at B_{QCP} in Fig. 1, which is equivalent to a divergency in A and a singularity in the electronic density of states $g(\varepsilon_F) \approx 2/3\varepsilon_F$ per electron at ε_F. Such a singularity is energetically unfavorable, because the potential gain in free energy $F \approx -g(\varepsilon_F)\Delta^2/2$ caused by the opening of a gap 2Δ upon formation of an ordered phase depends on $g(\varepsilon_F)$. The extrapolated fit to $A^{-1/2}$ is plotted as A in Fig. 3 for the $x = 4\%$ sample, for which the HO phase is absent. Rather than continuing to diverge at B_{QCP}, as predicted by the fits of A to $A \propto |B - B_{QCP}|^{\alpha}$ (note the logarithmic scale), actual values of A [and therefore also $g(\varepsilon_F)$] fall to a local minimum within phase II, indicating that its formation is effective at mitigating quasiparticle divergences. Such a reduction in A is consistent with a scenario in which the formation of phase II lowers the total energy of the system in avoiding the QCP by opening a partial gap at ε_F. This was one of several possibilities considered to account for a drop in A close to B_M in $Sr_3Ru_2O_7$ at low temperatures [22]. In URu_2Si_2, the actual existence of new phases is confirmed by the thermodynamic verifica-

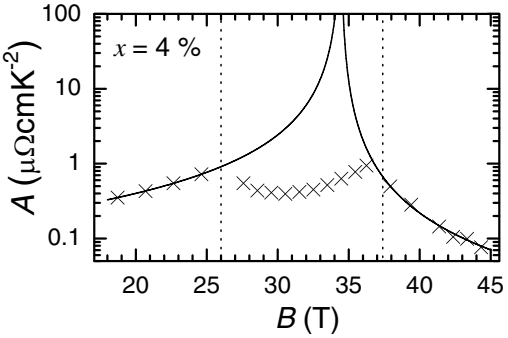

FIG. 3. Plot of A versus B for $x = 4\%$, with fits to the function $A \propto |B - B_{QCP}|^{\alpha}$ in the regions outside phase II, which is enclosed between dotted lines.

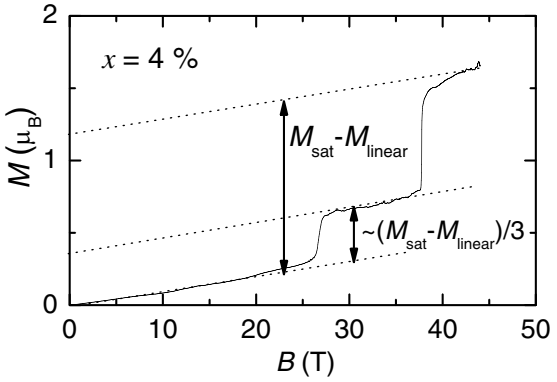

FIG. 4. Plot of the magnetization M measured in the $x = 4\%$ sample at 1.5 K. M for phase II is approximately one-third of $M_{\rm sat} - M_{\rm linear}$, where $M_{\rm linear}$ is a linear background magnetization due either to Pauli paramagnetism of the itinerant carriers or van Vleck paramagnetism.

tion of phase transitions in the magnetization [14] and specific heat [17].

An important finding in the present study is that we can unambiguously eliminate the HO parameter as being responsible for quantum criticality, since this phase is absent for $x = 4\%$. The close proximity of the HO phase does nevertheless add to the complexity of the phase diagram for $x < 3\%$ in Fig. 1. Whereas the HO parameter becomes rapidly weakened on doping with Rh, phase II is robust and may even become slightly strengthened. Phase III (considered as a possible reentrant HO [14]) suffers a similar fate to the HO. It is further interesting to note that M within phase II acquires a value that is approximately one-third of the saturated value above 38 T, upon taking into consideration the background linear slope in Fig. 4. A qualitatively similar one-third magnetization state is observed in UPd_2Si_2, which is proposed to be a system where the staggered $5f$ moments are in a Γ_5 Ising doublet configuration [19]. A low energy Fwithin phaseΓ_5 doublet has been proposed to give rise to competing antiferromagnetic and antiferroquadrupolar phases in URu_2Si_2 at low magnetic fields (the latter also being a candidate for the HO parameter) [19,28], and a heavy-Fermi-liquid (i.e. Kondo singlets) in the absence of order.

In the present study, we conclude that phase II likely forms as a means of avoiding quasiparticle divergencies that would otherwise occur at a magnetic field-tuned QCP. Supporting evidence includes the quenching of $A \propto g(\varepsilon_{\rm F})^2$ within phase II in Fig. 3, and the common trend in $B_{\rm QCP}$, $B_{\rm II}$, and $B_{\rm M}$ as a function of x. The present results therefore identify $U(Ru_{1-x}Rh_x)_2Si_2$ as a promising candidate for establishing a causality link between field-tuned quantum criticality and the creation of novel field-induced phases.

This work is supported by the National Science Foundation, by the Department of Energy, and by Florida State. We thank Christian Batista for useful discussions. K. H. K. thanks M. Cho and the KOSEF through CSCMR. One of the authors (N. H.) thanks Qimiao Si for useful discussions.

Note added.—The raw data pertaining to Fig. 1 have been archived [29].

*Present address: CSCMR & School of Physics, Seoul National University, Seoul 151-742, Korea.

[1] R. B. Laughlin *et al.*, Adv. Phys. **50**, 361 (2001).
[2] S. Sachdev, Science **288**, 475 (2000).
[3] H. Löhneysen, J. Magn. Magn. Mater. **200**, 532 (1999).
[4] R. Roussev and A. J. Millis, Phys. Rev. B **63**, 140504(R) (2001).
[5] C. M. Varma, Phys. Rev. B **55**, 14 554 (1997).
[6] E. Pugh, Philos. Trans. R. Soc. London A **361**, 2715 (2003).
[7] N. D. Mathur *et al.*, Nature (London) **394**, 39 (1998).
[8] S. S. Saxena *et al.*, Nature (London) **406**, 587 (2000).
[9] J. L. Tallon, J.W. Loram, and C. Panagopoulos, J. Low Temp. Phys. **131**, 387 (2003).
[10] P. Coleman *et al.*, J. Phys. Condens. Matter **13**, R723 (2001).
[11] A. J. Millis *et al.*, Phys. Rev. Lett. **88**, 217204 (2002).
[12] S. Chakravarty *et al.*, Phys. Rev. B **63**, 094503 (2001).
[13] K. H. Kim *et al.*, Phys. Rev. Lett. **91**, 256401 (2003).
[14] N. Harrison, M. Jaime, and J. A. Mydosh, Phys. Rev. Lett. **90**, 096402 (2003).
[15] A. Suslov *et al.*, Phys. Rev. B **68**, 020406(R) (2003).
[16] N. Shah *et al.*, Phys. Rev. B **61**, 564 (2000); P. Chandra *et al.*, Nature (London) **417**, 881 (2002).
[17] M. Jaime *et al.*, Phys. Rev. Lett. **89**, 287201 (2002).
[18] J. S. Kim *et al.*, Phys. Rev. B **67**, 014404 (2003).
[19] H. Amitsuka *et al.*, in *Proceedings of the 4th International Symposium on Advanced Critical Fields, Tsukuba, 1999* (NRIM, Tsukuba, 1999), p. 29.
[20] M. Yokoyama *et al.*, J. Phys. Soc. Jpn. **73**, 545 (2004).
[21] Maxima can also occur at second order ferromagnetic transitions, when sample size or demagnetizing effects become important.
[22] S. A. Grigera *et al.*, Science **294**, 329 (2001).
[23] S. Sachdev, *Quantum Phase Transitions* (Cambridge University Press, Cambridge, 1999).
[24] K. Kadowaki and S. B. Woods, Solid State Commun. **58**, 507 (1986).
[25] H. Ohkuni *et al.*, Philos. Mag. B **79**, 1045 (1999); the published Fermi surface data for semimetallic URu_2Si_2 yields $\aleph \sim 1.6\%$ for $B \lesssim 20$ T and $T < T_{\rm O}$. Because the extent of a possible change at $T_{\rm O}$, $B_{\rm M}$, or $B_{\rm QCP}$ is presently unknown, this number can be considered only for order of magnitude estimates elsewhere in the phase diagram.
[26] H. Aoki *et al.*, Phys. Rev. Lett. **71**, 2110 (1993).
[27] T. Senthil, S. Sachdev, and M. Vojta, Phys. Rev. Lett. **90**, 216403 (2003); T. Senthil, M. Vojta, and S. Sachdev, Phys. Rev. B **69**, 035111 (2004).
[28] H. Amitsuka *et al.* (to be published).
[29] K. H. Kim, N. Harrison, H. Amitsuka, G. A. Jorge, M. Jaime, and J. A. Mydosh, cond-mat/0411068.